Spectroscopic Analysis of Ordering and Phase-Separation Behavior of Model Polyurethanes in a Restricted Geometry

Curtis W. Meuse,[†] Xiaozhen Yang, Decai Yang, and Shaw L. Hsu[*]

Polymer Science and Engineering Department, University of Massachusetts, Amherst, Massachusetts 01003

Received August 12, 1991; Revised Manuscript Received October 14, 1991

ABSTRACT: Ultrathin films (40–300 Å) of model polyurethanes with monodisperse hard segments were studied as a function of film thickness and sample preparation. External-reflection infrared spectroscopy incorporating the double-modulation technique was used to characterize the phase-separation behavior of these copolymers into hard-segment-rich or soft-segment-rich domains. Using the C═O stretching or N–H in-plane-bending vibrations, vibrational spectroscopy can independently probe the localized hydrogen-bonding environment and the orientation of the hard segments in both domains. For anisotropic ultrathin films studied by reflection spectroscopy, the band intensities observed represent the degree of phase separation as well as the orientation of the urethane groups on the substrate. A procedure was developed to separate effects arising in phase separation from those related to segmental orientation. On solid surfaces, the results indicate that the amount of orientation and degree of phase separation observed is controlled by the film thickness. Annealing studies reveal that the reduced mobility of the polyurethanes on the surface prevents the thin films from achieving degrees of phase separation similar to those observed in the bulk. Glycerin is expected to have a specific interaction with the polyurethane, and the microstructure of a thin polyurethane film cast on a glycerin surface is different from that of thin films cast on gold. The increased mobility of polyurethanes on glycerin allows a higher degree of phase separation to be achieved. In addition, upon annealing on the surface of glycerin, transmission electron microscopy reveals changes in aggregation of the hard domains, while spectroscopy shows orientation changes.

Introduction

Polyurethanes are multiblock copolymers usually consisting of aromatic hard segments and polyether or polyester soft segments. These polymers have very attractive bulk mechanical properties due to the presence of phase-separated structures.[1-6] The surface properties and the associated structures of polyurethane are extremely important for its use in applications such as medical implants, membranes, adhesives, and coatings. Studies utilizing X-ray photoelectron spectroscopy (XPS), attenuated total reflection spectroscopy (ATR), scanning electron microscopy (SEM), contact angle measurements, and other techniques have determined that the segmental composition of the surface and the bulk of the polyurethane can be quite different.[7-13] The flexible segments of the polyurethane have a lower surface energy and preferentially aggregate at the surface.[10] The degree of preferential aggregation is related to the ratio of hard to soft segment present in the polymer, the casting solvent, the substrate, and the temperature and rate at which the polymer film is prepared.[7-14] These studies also report that steric and conformational factors dominate the thermodynamic driving force that attempts to reduce the interfacial energy at the polymer surface.[11] A relatively small number of studies have been directed at ultrathin films compared to the number on polyurethane surfaces.[15-18] Characterization of the structure of ultrathin films would extend our knowledge of the polymer surface because both the surface and the thin film confine the polyurethane to an air–polymer interface. The principal objectives of this study are to determine the degree of phase separation and the orientation of the hard segments in both domains of very thin polyurethane films.

The factors governing the structure formation in a restricted geometry are unknown, and the transition from the bulk to the thin film structure is unclear. Intuitively, the degree of phase separation and the orientation of the phase-separated domains is expected to be dependent on the length of the hard segments. Theory predicts that the orientation caused by the surface would only affect the first three or four layers from the interface between the air and the polymer.[19-22] Vibrational spectroscopy has been often used to characterize the degree of phase separation and segmental orientation of polyurethanes in the bulk state.[5,6,23-31] In order to characterize these ultrathin films, an extremely high sensitivity is necessary. Infrared reflection–absorption spectroscopy with polarization modulation has recently been used to observe the orientation of adsorbed polystyrene/poly(propylene sulfide) copolymers in this laboratory.[32] Polyurethane films with their low packing density of urethane groups also require this technique in order to probe orientation, conformation, and aggregation.

For polyurethanes, vibrations such as C═O stretching or N–H in-plane bending are characteristic of the localized hydrogen-bonding environment.[5,6,23-31] In addition, when polarization characteristics are known, both the degree of phase separation and the orientation can be independently probed using vibrational spectroscopy. Double-modulated external reflection has recently been used to measure films as thin as 10 Å,[32] much thinner than the expected thickness of the polyurethane used in this work. In this study, the orientation and phase separation of these molecules is determined as a function of the thickness of the cast film and of the substrate on which the polymer is cast. Since the thickness of the film is on the order of the length of the hard segment of the polyurethane,[5,6] the thickness of the film and the interactions of the substrate should directly influence the way the hard segments orient and how these phase separate.

---

[*] To whom correspondence should be addressed.

[†] Department of Chemistry.

0024-9297/92/2225-0925$03.00/0

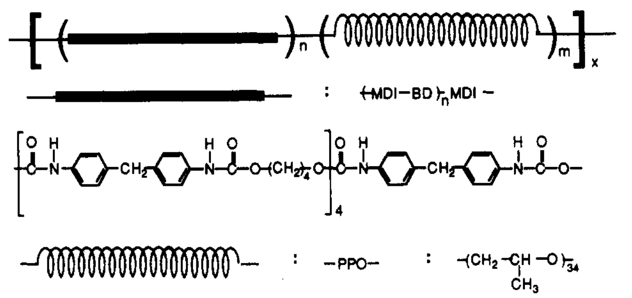

Figure 1. Schematic drawing of the model polyurethane used in this study ($n = 4$ corresponds to B4 polymer).

Experimental Section

The polyurethane used in this study has been described previously.[5] It contained monodisperse methylenebis(phenyl isocyanate) (MDI)–butanediol (BD) hard segments and poly(propylene oxide) (PPO; Voranol TM, molecular weight 2000) soft segments. In this polyurethane, there are five MDI units connected by four butanediol groups; thus, the polymer is designated B4 in Figure 1.

The B4 polymer was coated on an evaporated gold film supported on a Fisherbrand glass microscope slide (25 × 25mm) that had been cleaned with acetone, distilled deionized water, ethanol, and 2:1 H_2SO_4–H_2O_2 (*Caution*! piranha acid, 2:1 H_2SO_4–H_2O_2, can react violently with organic materials) and stored in ethanol. The ethanol was removed from the slide with nitrogen just prior to coating the slide. The gold (99.998% gold wire, Alfa or Johnson Matthey, 0.5 mm) was evaporated from resistively heated tungsten baskets in a modified Balzers MED 010 vapor deposition apparatus with a base pressure of 1×10^{-6} mm. The gold was coated to a minimum thickness of 1800 Å as monitored by a quartz-crystal thickness monitor.

The polyurethane films to be studied were cast by depositing a known amount of dimethylformamide (DMF) or tetrahydrofuran (THF) solution of known polymer concentration onto the substrate. The ratio of polymer volume to area is used to estimate the thickness of the film. For the films cast onto gold, the vacuum desiccator was slowly evacuated over 4 h as the solvent evaporated to an ultimate pressure of 25 mmHg. The samples were dried under vacuum for 8 h more until any remaining solvent was removed. The complete removal of solvent was verified by the lack of outgassing when the samples were introduced to the UHV chamber of the XPS. The samples were transferred directly from the drying desiccator to the nitrogen-purged sample chamber of the Nicolet 60SXB FT-IR spectrometer.

Thin films were also prepared by casting on glycerin from solutions of 2.6 or 5.0 mg/mL of B4 polyurethane in THF. In contrast to the gold or carbon surfaces (for transmission electron microscopy [TEM]), glycerin is expected to have strong secondary interactions with the polymer. In addition, solutions on glycerin surfaces cast continuous films that could be studied with standard TEM techniques. The glycerin was heated to about 60 °C, and the film was then lifted from the glycerin and placed in water at the same temperature to remove the glycerin. The film could then be moved to either copper grids or gold surfaces for characterization. The thickness of the samples was also studied using a Rudolph autonulling ellipsometer. The values are an average of at least five different spots on the surface of the sample.

An infrared spectrum obtained for an isotropic polyurethane film is shown in Figure 2. In this same figure, spectra obtained for 80- and 160-Å-thick polyurethane films are shown as well. External-reflection infrared spectra were obtained using polarization modulation as described previously.[32] All spectra were obtained with a Nicolet 60SXB FT-IR equipped with a liquid-nitrogen-cooled MCT detector at a resolution of 2 cm^{-1}. The external-reflection double-modulation measurements required 512 scans whereas the external-reflection background and transmission measurements required 64 scans. It should be emphasized that spectroscopic data of acceptable signal-to-noise ratio could not be obtained without the double-modulation technique. It is clear that the relative intensities of the bands obtained by two different spectroscopic techniques are quite different. Virtually all well-defined bands such as C=O stretching and N–H in-plane-bending vibrations in the 1700- and 1500-cm^{-1} regions, respectively, exhibit dramatic intensity differences. Previous spectroscopic studies of polyurethanes generally invoke the two-phase model. The doublet in the C=O stretching region (~1700 cm^{-1}) is taken to represent a hydrogen-bonded component and a free one. The hydrogen-bonded component can only exist in the hard domains. The free component exists only dispersed in the soft phase. We have not observed any unusual spectroscopic features associated with the hydrogen properties of these samples in the thin films. It should be emphasized that, because of the high anisotropy associated with the thin films, the relative band intensities need to be carefully analyzed before any definite conclusions regarding the degree of phase separation and segmental orientations can be deduced.

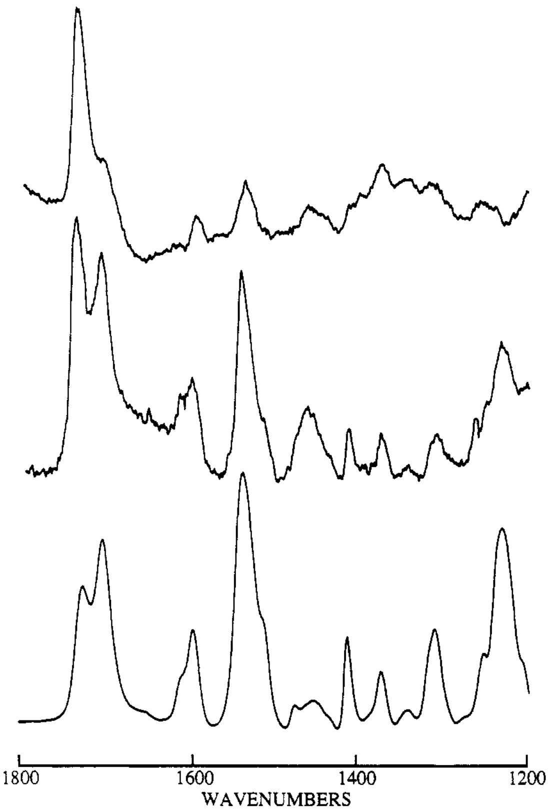

Figure 2. Infrared spectra (spectral resolution = 2 cm^{-1}) obtained for 80-Å, 160-Å, and isotropic polyurethane films. The top two spectra were obtained by the external-reflectance technique incorporating double-modulation spectroscopy; 512 scans were coadded in each case. The spectrum obtained for the isotropic film is obtained by the transmission technique; 64 scans were coadded.

The relative surface energies of the systems were characterized by dynamic contact angle measurements made by a Rame-Hart telescopic goniometer using water added by a Gilmont syringe. The measurements were taken as the water was being added (θ_A) or removed (θ_R). The surfaces designated as "washed" were washed three times with 1 mL of ethanol (USP absolute 200 proof from Aaper Alcohol and Chemical Co.) and blown dry (Aero-Duster). The contact angles of the washed surfaces were taken within 4 min of the beginning of the drying procedure, and the values reported are averages of measurements from two washes taken at six different places on the surface. Transmission electron microscopy (TEM) was done on a JEOL 100 CX transmission electron microscope operated at 100 kV.

The X-ray photoelectron spectra were obtained using a Perkin-Elmer Physical Electronics 5100 with Mg Kα excitation (300 W, 15 keV). The take-off angle reported is the angle between the film surface and the analyzer. Survey spectra were taken with pass energy of 89 eV and an acquisition time of 5 min. The atomic ratios were determined using Physical Electronics software and programmed sensitivity factors for multiplexed spectra

Table I
Advancing Contact Angle (θ_a) Data of Films with Different Thicknesses (Thickness from Concentration Only)

	θ_a before EtOH wash, deg	θ_a after EtOH wash, deg		θ_a before EtOH wash, deg	θ_a after EtOH wash, deg
uncoated gold	100	60	160 Å	88	86
			170 Å	82	80
50 Å	81	70	210 Å	83	82
80 Å	85	87	270 Å	81	82
100 Å	90	80	bulk film	86	85

obtained with a pass energy of 35.75 eV and a 10-min acquisition time.

Results and Discussion

The first step is to characterize the geometry of the ultrathin films using angle-resolved XPS ellipsometry and contact angle measurements. Continuous films are expected to provide a more representative model of the polyurethane surface than polymer islands on a gold surface. XPS and infrared samples are characterized in parallel, due to the limited area in the ultrahigh vacuum chamber of the XPS and the larger infrared samples. For a continuous film studied by XPS, the sine of the emergence angle is linearly related to the intensity of the gold peak.[32,33] This method indicated that polyurethane films as thin as 40 Å could be continuous. Contact angle measurements allowed the film to be characterized independent of the size of the sample. The relative surface energies of the samples can be measured by contact angle, using the XPS samples as references. The angles measured for polyurethane (advancing, 88°; receding, 45°) are not much different from those obtained for gold (advancing, 90°; receding 50°). However, the values for gold are much different from the reported values of 0–8° for absolutely clean gold.[34] The discrepancy for gold is due to the adsorption of hydrocarbons from the air. When gold was washed (three times with 1 mL of ethanol), the values decreased to 60° advancing and 15° receding. These values agree nicely with values reported by Whitesides for a similarly washed system.[35] The ethanol wash removes some of the hydrocarbons and/or puts down a layer of ethanol on the surface. For the samples that XPS results suggest are continuous polyurethane, the contact angles do not change after the ethanol wash. Using this technique, the continuity of the larger infrared samples can be easily confirmed. Typical results are summarized in Table I. The thickness of the films judged to be continuous is determined from knowing the concentration cast onto a known area and by ellipsometry. The films that had holes by the contact angle measurements did not give reproducible thickness measurements by ellipsometry. Neither surface coverage nor thickness could be determined for films with holes.

Determination of the Degree of Phase Separation and Orientation of the Hard Segment in Both Domains. The principal objective of this study is to examine the degree of phase separation and the associated orientation changes for polyurethanes in restricted geometries. This analysis is based on the fact that strong interurethane hydrogen bonds only are formed for the phase-separated domains.[5,6,23-31] The spectra obtained by the reflectance technique contain all the features generally used to characterize polyurethanes. Several vibrations, such as C=O stretching and N–H in-plane bending, are perturbed by the formation of hydrogen bonds.[6] The degree of phase separation can be derived from the relative intensity of the hydrogen-bonded C=O stretching at ~1700 cm^{-1} versus the 1735-cm^{-1} component representing C=O dispersed in the soft matrix (Figure 2). In most previous polyurethane studies, a two-phase approximation is used to describe the hydrogen-bonded environment. This analysis is straight-forward for isotropic films. For anisotropic ultrathin films studied by external reflection, however, the dramatically different relative intensities observed as compared to the isotropic film represent the degree of phase separation as well as the orientation of the urethane groups on the substrate. The procedures for obtaining reflection data and for determining segmental orientation of anisotropic films have been described previously.[32,35-38] A procedure for separating effects arising in phase separation from those related to segmental orientation follows.

For isotropic materials, the ratio of the absorbances is

$$\frac{A_b}{A_f} = \left(\frac{\kappa_b}{\kappa_f}\right)\frac{X}{1-X} \tag{1}$$

where the absorbances of the hydrogen-bonded and free vibrations are represented by A_b and A_f, respectively. The degree of phase separation is represented X, and the absorptivities are κ_b and κ_f. For the data obtained by the reflection experiment for anisotropic films, the absorptivities also have components due to orientation described by their orientation factors P_b and P_f.

$$\frac{A_b}{A_f} = \left(\frac{\kappa_b P_b}{\kappa_f P_f}\right)\frac{X}{1-X} \tag{2}$$

There are four equations describing all the possible absorbances:

$$A_b = \kappa_b P_b X \tag{3}$$

$$A'_b = \kappa'_b P'_b X \tag{4}$$

$$A_f = \kappa_f P_f (1-X) \tag{5}$$

$$A'_f = \kappa'_f P'_f (1-X) \tag{6}$$

In these expressions, the variables containing a prime are related to the N–H in-plane bending and those without are associated with C=O stretching. The two components of N–H in-plane bending are not resolved. The expressions describing the relative absorbances are then

$$\frac{A'_b + A'_f}{A_b} = \frac{\kappa'_b}{\kappa_b}\left(\frac{P'_b}{P_b}\right) + \frac{\kappa'_f}{\kappa_b}\left(\frac{P'_f}{P_b}\right)\frac{1-X}{X} \tag{7}$$

$$\frac{A'_b + A'_f}{A_f} = \frac{\kappa'_b}{\kappa_f}\left(\frac{P'_b}{P_f}\right)\frac{X}{1-X} + \frac{\kappa'_f}{\kappa_f}\left(\frac{P'_f}{P_f}\right) \tag{8}$$

In order to obtain values that are independent of sample thickness, ratios of the absorbances are used. Eliminating the $X/(1-X)$ term, there follows

$$\frac{A'_b + A'_f}{A_f} = \frac{\kappa'_b}{\kappa_b}\left(\frac{P'_b}{P_b}\right)\frac{A_b}{A_f} + \frac{\kappa'_f}{\kappa_f}\left(\frac{P'_f}{P_f}\right) \tag{9}$$

$$\frac{A'_b + A'_f}{A_b} = \frac{\kappa'_b}{\kappa_b}\left(\frac{P'_b}{P_b}\right) + \frac{\kappa'_f}{\kappa_f}\left(\frac{P'_f}{P_f}\right)\frac{A_f}{A_b} \tag{10}$$

The ratios of the κ's can be obtained from spectra of an isotropic film undergoing phase separation.[6] This ratio was 1 if measured by the total area,[6] and if by peak heights, the ratio was 1.05. A range of values from 1.00 to 1.70 has been reported for the relative absorptivity for the bonded versus free species.[23-31] If $(A'_b + A'_f)/A_b$ is plotted against A_f/A_b or $(A'_b + A'_f)/A_f$ is plotted against A_b/A_f, then the ratios of κ'_f/κ_f and κ'_b/κ_b can be obtained from both eqs 11 and 12.

$$\frac{A'_b + A'_f}{A_b} = \frac{\kappa'_b}{\kappa_b} + \frac{\kappa'_f}{\kappa_f}\frac{A_f}{A_b} \tag{11}$$

$$\frac{A'_b + A'_f}{A_f} = \frac{\kappa'_f}{\kappa_f} + \frac{\kappa'_b}{\kappa_b}\frac{A_b}{A_f} \tag{12}$$

Once these ratios are found, the absorbances from the thin films have only three unknown values (X, P_f's, and P_b's) described by three equations (eqs 2, 9, and 10). If the equations that do not involve the degree of phase separation (eqs 9 and 10) are solved first, the ratios of the orientation factors for both the bonded and the free domains can be obtained.

The relationship between P and P' can be derived explicitly. The transition dipole moment for the C=O stretching vibration is ~78° with respect to the chain axis.[39] The N–H in-plane bending of the amide has a transition moment at 68° with respect to the C–N bond,[40] which is nearly parallel to the chain axis in the polyurethanes. The fact that these two transitions are nearly perpendicular to each other is used to calculate the orientational distribution functions of the bonded and free species.

To calculate the orientation of individual transition moments, recall that, for an electromagnetic wave of infrared radiation interacting with a transition moment, the absorptivity, a, for all orientations, can be expressed by eq 13 where M_0 is the change in the transition moment

$$a \propto E^2 M_0^2 \int_0^{2\pi}\int_0^{\pi} f(\theta,\phi)\cos^2\theta \sin\theta \, d\theta \, d\phi \tag{13}$$

during a vibration and $f(\theta,\phi)$ is the distribution function of transition moments. The orientation factor can be illustrated schematically by considering a transition moment M_0 that has components M_x, M_y, and M_z in the three Cartesian directions. The sum of the squares of the fractional transition moments, i.e. $(M_x^2 + M_y^2 + M_z^2)/M_0^2$, is 1. Define $D_x = M_x^2/M_0^2$, $D_y = M_y^2/M_0^2$, and $D_z = M_z^2/M_0^2$. Then $D_x + D_y + D_z = 1$. From the approximate geometric relationship between C=O stretching and N–H in-plane-bending vibrations

$$D_x' = D_y/2 + D_z/2 \tag{14}$$

$$D_y' = D_x/2 + D_z/2 \tag{15}$$

$$D_z' = D_x/2 + D_y/2 \tag{16}$$

In the reflection experiment, because of the boundary conditions near the metallic surface, only the component parallel to the surface normal can be observed.

Since there is no preferential orientation in the plane of the film

$$D_z' = (1 - D_z)/2 \tag{17}$$

On the basis of the normalization factor required for eqs 3–6, define $P = 3D_z$ and $P' = 3D_z'$. Then

$$P' = (3 - P)/2 \tag{18}$$

or

$$P = (3 - P')/2 \tag{19}$$

Table II
Degree of Phase Separation and the Orientation of the Hard Segments in Both Domains in the As-Cast Samples

	X, %	f_{free}	f_{bonded}
	Cast on Gold		
80 Å	24	0.46	0.16
160 Å	48	0.16	0.09
	Cast on Glycerin		
170 Å cast on glycerin	61	0.04	0.16
210 Å annealed on gold	61	0.04	0.16
270 Å annealed on glycerin	61	−0.09	0.11

Since only one experimental value is available, i.e., the ratio between the band intensity of C=O stretching and N–H in-plane-bending vibrations

$$P'/P = \alpha \tag{20}$$

there is no unique solution. Instead, two possible sets of values are obtained

$$P = \frac{3}{2\alpha + 1} \quad \text{and} \quad P' = \frac{3\alpha}{2\alpha + 1} \tag{21}$$

or

$$P = \frac{3}{\alpha + 2} \quad \text{and} \quad P' = \frac{3\alpha}{\alpha + 2} \tag{22}$$

The differences between the two sets of solutions in most cases are quite clear. Since the analysis does not allow a determination of which of the two values calculated is correct, the orientation behavior can be calculated using the average of the two. The closer to isotropic the system is, the smaller the error in the calculation.

These values of P and P' can then be obtained for both the hard- and soft-segment-rich domains. The average angle of deviation between transition moment and the surface normal can then be obtained

$$\theta = \cos^{-1}\sqrt{(P/3)^{1/2}} \tag{23}$$

Once the orientation is known, the P's can be used to calculate the degree of phase separation X in eq 2.

Segmental Orientation and Phase-Separation Behavior as a Function of Sample Thickness. The morphology of thin polyurethane films exhibits significant differences in the degree of phase separation and segmental orientation, depending on film thickness and sample preparation. These results are summarized in Table II. Positive values indicate chains that are oriented parallel to the surface, since the transition moment of the urethane carbonyl is at a 78° angle with respect to the chain backbone.[39] The definition of the transition moment direction of this vibration cannot be exact. There are more quantitative studies to define the transition moments in polypeptides and related model compounds.[41,42] In those studies, the transition moments defined for related bands are perhaps no better model than the one used in our paper, because the amide I (C=O stretching) and amide II (N–H in-plane bending) bands are perturbed by interchain interactions.[42] The less than precise definition of the transition moments, however, does not change the fact that dramatic differences observed in some films are due to segmental orientation effects.

After taking into account of segmental orientation, it is then possible to derive the amount of phase separation in each sample. This is shown in Figure 3. The data show, for films cast onto gold, the thinner films are more phase mixed and the hard segments in both domains are more oriented into the plane of the surface than in the thicker films. The hard segments in hard domains are less oriented than the hard segments dispersed in the soft segments in all film thicknesses. In the thin films, the polymer is

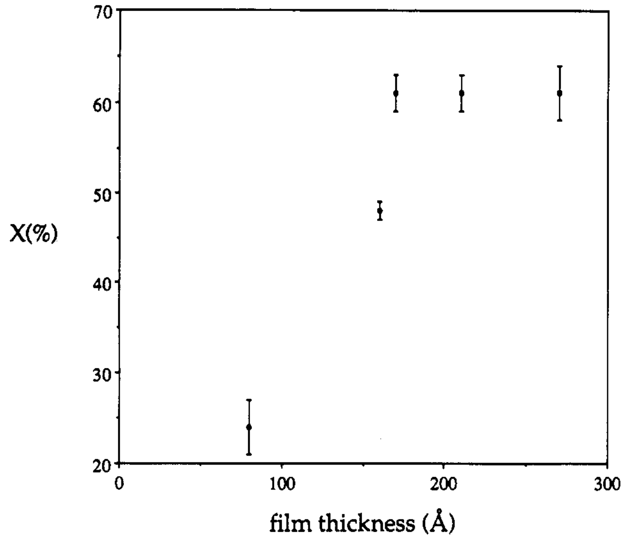

Figure 3. Degree of phase separation measured as a function of thickness for thin polyurethane films.

confined to a restricted geometry because the hard segments are longer than the film is thick. The height of this volume is defined by the air–polymer interface or the interface of the domain defined by the soft segments aggregated at the air–polymer interface. When confined, the polymer is forced into a higher energy state due to loss of translational entropy. It has been predicted that high segmental orientation exists at the air–polymer interface.[19–22] To relieve this loss of entropy or net increase of free energy, because hard segments are not sufficiently rigid to prevent conformational defects from being introduced. If there are defect hard segments, the urethane groups would be expected to be less oriented than for the straight hard-segment case, but the same general ideas would apply. The energy of the interface also changes the hydrogen bonding of the polyurethane, imparting a more phase-mixed structure on the surface.

In the initial state of an 80-Å film, only 24% of the urethane carbonyl is hydrogen bonded. Typically, in the bulk B4 polyurethane film around 55% of the urethane carbonyl might be hydrogen bonded.[5,6] This indicates that in the casting process there is very little opportunity for phase separation. Phase separation may occur either in solution or in the film-forming process. Once the solvent is removed, the mobility of the polymer is reduced and further phase separation restricted. In the solutions used to cast the 80- and 160-Å films, there may not be aggregation of the hard domains as the concentrations are very low and the polymer is dissolved in good solvents.[43] As the solvent is removed, the concentration increases and some micellization may occur.[44] The interchain hydrogen bonding is expected to be low, because, even in a planar geometry, the polymer is present in less than a hard segment length, allowing very little lateral interaction. While the solution is present, the polyurethane is expected to be able to form intramolecular hydrogen bonds. However, since the thinner films are less than the length of the hard segment, the interaction between chains in the plane of the film is not expected to be large and the degree of hydrogen bonding in the thin film is expected to be lower than that in the bulk, as is observed.

Analysis of the 80-Å thin film displayed in Table III indicates the initial state produced evolves to a more favorable state. Both the degree of phase separation and the orientation of the hard segments in both domains change. Initially, 24% of the urethane groups is hydrogen bonded and the orientation of the hard-segment-rich domains is 0.16 compared to 0.46 for the hard segments surrounded by soft segments. Over the course of 23 days, the hydrogen bonding increased to 34% and the orientation fell to 0.07 for the hard-segment-rich phase and to 0.34 for that in the soft-segment-rich phase. In the dry film, the limited mobility and small amount of lateral interaction of the polyurethane are expected to restrict the phase separation that slowly develops over 23 days.

Table III
Changes in the Films as a Function of Time and Annealing

time	X, %	$f_{\text{free C=O}}$	$f_{\text{H-bonded C=O}}$
	80-Å Film over Time		
1 day	24	0.46	0.16
5 days	33	0.43	0.18
23 days	34	0.34	0.07
	80-Å Film Annealed at 90 °C		
0 min	37	0.34	0.07
16 min	37	0.33	0.1
60 min	38	0.32	0.08
	80-Å Film Annealed at 120 °C		
0 min	38	0.32	0.08
5 min	42	0.24	0.07
10 min	44	0.26	0.12
	160-Å Film Annealed at 90 °C		
0 min	48	0.16	0.09
15 min	47	0.14	0.07
60 min	48	0.11	0.04

Since the 160-Å film is much closer to a monolayer, its lateral interactions and mobility are greater. The degree of phase separation shown in Table II is much greater than that of the 80-Å film. In addition, the structure of the 160-Å film did not change over the first 30 days after the film was cast. In both films, as the solvent is removed from the surface, the concentrations the casting solutions attain during the casting process must be similar. If the degree of phase separation achieved were determined by the amount of micellization in solution, then the degree of phase separation of the 80- and 160-Å films would be expected to be similar. Since this is not the case, this seems to indicate that most of the phase separation in the thin films happens as these are formed on the surface. Once the films are formed, the differences between the 80- and 160-Å films in terms of lateral interactions and mobility could cause the differences in orientation and phase separation that are observed. The greater degree of phase separation in the 160-Å film means the driving force for a secondary change in the structure is lower. In order to study the lateral interactions involved in these planar phase separations, annealing studies of the two films were undertaken.

Annealing. After the structure of the 80-Å film stabilized, it was annealed at 90 °C for up to 1 h. The spectra obtained for annealed samples are shown in Figure 4. It is quite evident that the N–H in-plane-bending band changes relative to the C=O stretching. Results summarized in Table III show that the orientation and degree of phase separation did not change. This may indicate that the orientation and degree of phase separation of the 80-Å film has reached a stable state in 23 days at room temperature. Since the hard segments are significantly oriented in the soft-segment-rich domain with an orientation function value of 0.32, the restriction imposed by the air–polymer interface keeps them from obtaining orientations similar to the hard segments in the hard-segment-rich domains. Unless the free hard segments can reorient as the hard segments do in the hard domains, greater hydrogen bonding cannot be achieved. When the 80-Å film is annealed at 120 °C, the loss of translational

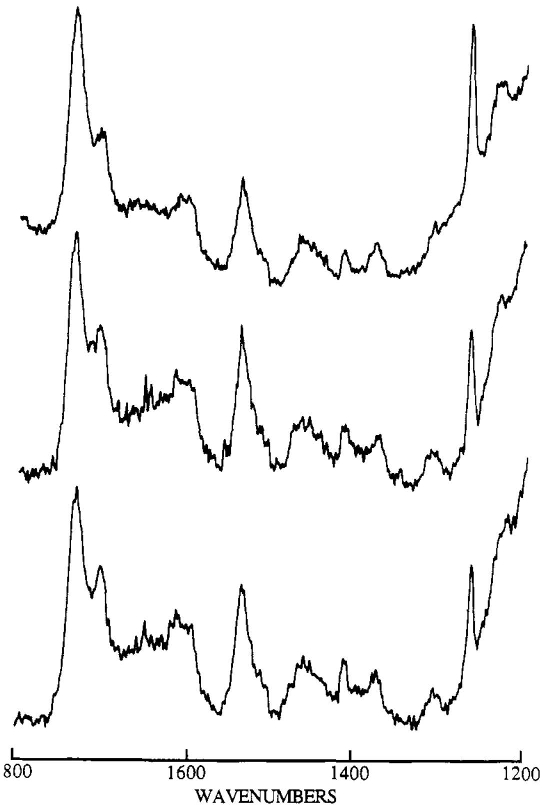

Figure 4. Reflectance infrared spectra obtained for thin films annealed at different time and temperatures: (top) annealed at 90 °C for 1 h; (middle) annealed at 120 °C for 5 min; (bottom) annealed at 120 °C for 10 min. Spectral resolution is 2 cm^{-1}; 512 scans are coadded.

energy becomes a large enough driving force to overcome the restricted mobility and lower degree of interpolymer interactions. This can be observed in the increase in the degree of phase separation and in the decrease in orientation of the hard segments in the soft-segment-rich domains. At 120 °C, in air, degradation of the polyurethanes is possible. This could explain the decrease of the orientation of the hard segments surrounded by soft segments. However, it would not explain the increase in the orientation of the hard segments in the hard-segment-rich domains or the increase of phase separation. A more likely explanation is that, with the increased driving force, the lateral interactions were once again able to cause phase separation in the plane of the thin film.

There is essentially no change in the degree of phase separation in the 160-Å film after annealing at 90 °C for 1 h, although there is some change in both orientation functions. In this case, 120 °C was not needed to drive orientation changes, which may be taken as an indication of increased mobility with increasing film thickness. If the hard segments can move but do not further phase separate, no further in-plane phase separation may be possible. The phase-separation mechanism proposed for polyurethanes is that of two-dimensional nucleation and growth, and the nucleation step has been shown to end at around 45% hydrogen bonded.[45] The growth step requires the polymers to migrate, something that is not possible in the thin films. As first cast, the 80-Å film had half the degree of phase separation of the 160-Å film, yet, after annealing, both systems developed similar degrees of phase separation. The two films have very different amounts of lateral interaction and restriction of orientation due to the air–polymer interface, but both of the most highly annealed 80- and 160-Å films have degrees of phase separation near 45%. The similar final degree of phase separation of the two films may be tied to the mobility of the polymers on the gold surface, indicating that the growth step has been prevented.

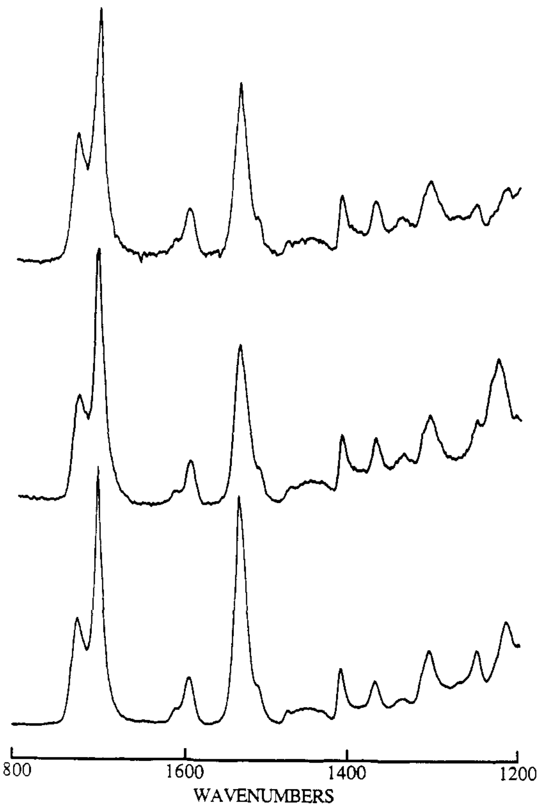

Figure 5. Reflectance infrared spectra obtained for thin films cast on glycerin and then annealed: (top) as cast; (middle) annealed on gold substrate at 90 °C for 1 h; (bottom) annealed on glycerin at 90 °C for 1 h.

Glycerin. The reflectance data obtained for the as-cast and annealed samples are shown in Figure 5. The results given in Table II show that the degree of phase separation is much higher for the samples cast on glycerin than for the films prepared on gold substrate. In contrast, the degree of hard-segment orientation in the hard domains is nearly the same for films of similar thickness, whether they are cast on gold or glycerin. The relative orientation of the hard segments in phase-separated domains also differs significantly from that of the hard segments in the soft-segment-rich domains. The degree of phase separation is higher because, even when the THF is evaporated, the polymers on glycerin still have a great deal of mobility that enhances phase separation. The increased mobility would also allow the soft-segment-rich domains, including hard segments, to reorganize even after the solvent evaporated. The lower degree of orientation of the hard segments in the soft domains compared to in the hard domains is evidence of this rearrangement.

The structure of a 170-Å-thick polyurethane film cast on glycerin and moved to a gold substrate exhibits high stability for annealing at 90 °C for 1 h. A considerable amount of structural reorganization occurred in samples annealed at 90 °C for 1 h on the glycerin surfaces. In this case, segmental orientation changed but the degree of phase separation did not. The process involved in the rearrangement upon annealing on glycerin is different from the process involved in the formation of the film because the area of the film decreases and the film thickness increases during annealing. While the difference in area is hard to quantitate, ellipsometric measurements indicate that the film thickness increases by 100 Å. The similar

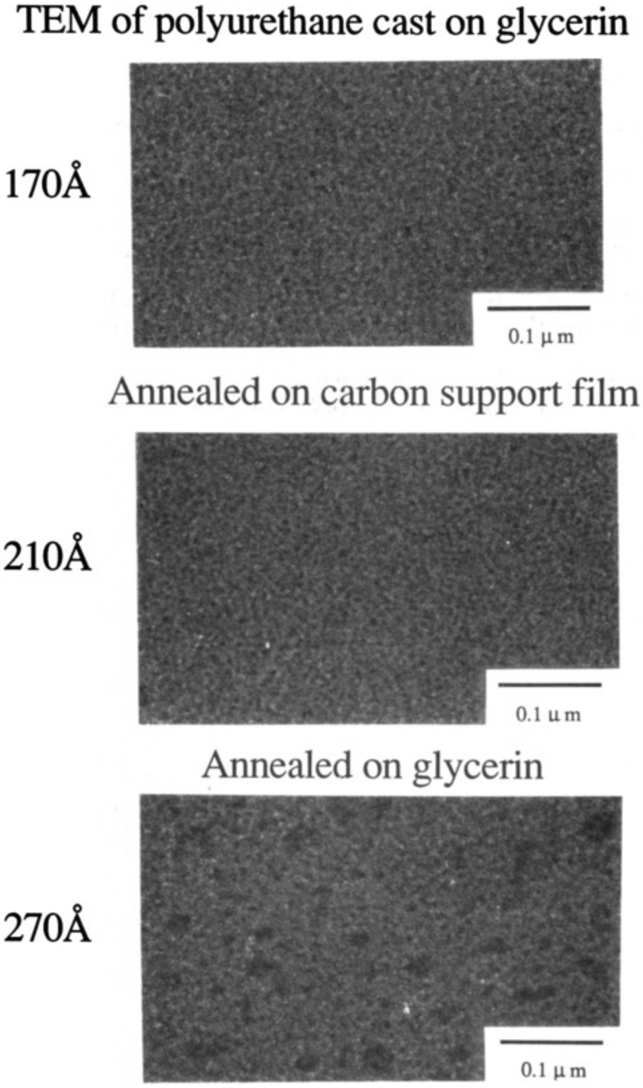

Figure 6. Transmission electron micrographs obtained for the as-cast and annealed polyurethanes.

degree of phase separation does not imply that additional structural rearrangements did not take place. In Figure 6, TEM shows another view of the phase-separation process. Initially, the hard domains observed are about 60 Å wide for polyurethanes cast on glycerin. For polyurethane annealed on a solid carbon film, which is analogous to annealing on the surface of gold, the domains are also approximately 60 Å wide. The film annealed on the surface of the glycerin has larger hard domains that are roughly 220 Å wide. The lack of mobility on gold or carbon substrates restricts the rearrangements the polyurethanes can undergo. However, with the increase in thickness and mobility on the surface of the glycerin, it was possible for the hard domains to aggregate to form larger hard domains that have less interfacial interaction with the soft domains.

The role of hydrogen bonding of the polymer with the glycerin surface is hard to determine. It might be expected that the soft segments would migrate preferentially to the surface even more in the thicker film. On the surface of the glycerin, the polyurethane film may be plasticized by the presence of the glycerin, especially at the elevated temperatures involved in the annealing process. The amount of the plasticization is hard to quantify, but angle-resolved XPS study shows that the surface composition of the polyurethane was similar before and after annealing. Annealing on the surface of gold changed the composition of the outermost layer more than annealing on glycerin. Therefore, plasticization is not a large effect.

The change in aggregation and the orientation of the polyurethane chain segments can be perturbed by a number of factors, including geometry. A summary of results for the ultrathin films prepared are shown in Figure 3. This plot and data listed in Table II show that the thinner films are significantly more phase mixed than the thicker ones. In both types of films prepared, i.e., cast onto inert surfaces such as gold and surfaces containing interacting groups such as glycerin, the phase separation and orientation of the hard segments in both domains change with differences in film thickness. The segmental orientation in these films are listed in Table II. These structural differences observed by infrared spectroscopy provide additional morphological information complementing other techniques described in earlier studies.

Conclusions

Very thin polyurethane films are influenced by the air–polymer interface. External reflection incorporating the double-modulation technique can be used to obtain the degree of phase separation and the amount of orientation of the hard segment in both the hard and soft domains of polyurethanes. The thin films are more phase mixed, and the hard segments in both domains are more oriented in the plane of the surface than are the bulk polyurethane films. Upon annealing, the excess phase mixing and orientation of the hard domains decreases the mobility on the surface and prevents further changes. In films cast on glycerin, the greater mobility allows higher degrees of phase separation and different orientations than in films cast on gold. Upon annealing, the hard domains aggregate causing differences in orientation and morphology. Infrared spectroscopy is useful for the study of orientation and the resulting morphology of thin polymer films.

References and Notes

(1) Cooper, S. L.; Tobolsky, A. V. *J. Appl. Polym. Sci.* **1966**, *10*, 1837.
(2) Samuels, S. L.; Wilkes, G. L. *Polym. Sci., Symp. C* **1973**, *43*, 149.
(3) Schneider, N. S.; Sung, C. S. P.; Matton, R. W.; Illinger, J. L. *Macromolecules* **1975**, *8*, 62.
(4) Koberstein, J. T.; Russell, T. P. *Macromolecules* **1986**, *19*, 714.
(5) Christenson, C. P.; Harthcock, M. A.; Meadows, M. D.; Spell, H. L.; Howard, W. L.; Creswick, M. W.; Guerra, R. E.; Turner, R. B. *J. Polym. Sci., Polym. Phys. Ed.* **1986**, *24*, 1401.
(6) Lee, H. S.; Wang, Y. K.; Hsu, S. L. *Macromolecules* **1987**, *20*, 2089.
(7) Takahara, A.; Tashita, J.; Kajiyama, T.; Takayanagi, M.; MacKnight, W. J. *Polymer* **1985**, *26*, 978.
(8) Takahara, A.; Tashita, J.; Kajiyama, T.; Takayanagi, M.; MacKnight, W. J. *Polymer* **1985**, *26*, 987.
(9) Lelah, M. D.; Grasel, T. G.; Pierce, J. A.; Cooper, S. L. *J. Biomed. Mater. Res.* **1986**, *20*, 433.
(10) Hu, C. B.; Sung, C. S. P. *Polym. Prepr. (Am. Chem. Soc., Div. Polym. Chem.)* **1980**, *21* (1), 156.
(11) Yoon, S. C.; Ratner, B. D. *Macromolecules* **1986**, *19*, 1068.
(12) Yoon, S. C.; Ratner, B. D. *Macromolecules* **1988**, *21*, 2392.
(13) Yoon, S. C.; Ratner, B. D. *Macromolecules* **1988**, *21*, 2401.
(14) Vargo, T. G.; Hook, D. J.; Gardella, J. A., Jr.; Eberhardt, M. A.; Meyer, A. E.; Baier, R. E. *Appl. Spectrosc.* **1991**, *45*, 448.
(15) Koutsky, J. A.; Hien, N. V.; Cooper, S. L. *J. Polym. Sci., Polym. Lett. Ed.* **1970**, *8*, 353.
(16) Fridman, I. D.; Thomas, E. L. *Polymer* **1980**, *21*, 388.
(17) Briber, R. M.; Thomas, E. L. *J. Macromol. Sci., Phys.* **1983**, *B22*, 509.
(18) Li, C.; Cooper, S. L. *Polymer* **1990**, *31*, 3.
(19) Helfand, E. *J. Chem. Phys.* **1975**, *63*, 2192.
(20) Yoon, D. Y.; Flory, P. J. *Macromolecules* **1984**, *17*, 868.
(21) Theodoro, D. N. *Macromolecules* **1988**, *21*, 1411.
(22) Theodoro, D. N. *Macromolecules* **1988**, *21*, 1422.
(23) Estes, G. M.; Seymour, R. W.; Cooper, S. L. *Macromolecules* **1971**, *4*, 452.
(24) Seymour, R. W.; Allegrezza, A. E., Jr.; Cooper, S. L. *Macromolecules* **1973**, *6*, 896.

(25) Seymour, R. W.; Cooper, S. L. *J. Polym. Sci., Part C* **1974**, *46*, 69.
(26) Seymour, R. W.; Cooper, S. L. *Rubber Chem. Technol.* **1974**, *47*, 19.
(27) Ishihara, H.; Kimura, I.; Saito, K.; Ono, H. *J. Macromol. Sci., Phys.* **1974**, *B10*, 591.
(28) Schneider, N. S.; Sung, C. S. P. *Macromolecules* **1975**, *8*, 68.
(29) Brunette, C. M.; Hsu, S. L.; MacKnight, W. J. *Macromolecules* **1982**, *15*, 71.
(30) Lin, S. B.; Hwang, K. S.; Tray, S. Y.; Cooper, S. L. *Colloid Polymer Sci.* **1985**, *263*, 128.
(31) Coleman, M. M.; Lee, K. H.; Skrovanek, D. J.; Painter, P. C. *Macromolecules* **1986**, *19*, 2149.
(32) Waldman, D. A.; Kolb, B. U.; MacCarthy, T. J.; Hsu, S. L., submitted for publication in *Langmuir*.
(33) Clark, D. T. *Adv. Polym. Sci.* **1977**, *24*, 125.
(34) Smith, T. *J. Colloid Interface Sci.* **1980**, *75*, 546.
(35) Troughton, E. B.; Bain, C. D.; Whitesides, G. M.; Nuzzo, R. G.; Allara, D. L.; Porter, M. D. *Langmuir* **1988**, *4*, 365.
(36) Allara, D. L.; Swalen, J. D. *J. Phys. Chem.* **1982**, *86*, 2700.
(37) Debe, M. K. *J. Appl. Phys.* **1984**, *55*, 3354.
(38) Umemura, J.; Kamata, T.; Kawai, T.; Takenaka, T. *J. Phys. Chem.* **1990**, *94*, 62.
(39) Zbinden, R. *Infrared Spectroscopy of High Polymers*; Academic Press: New York, 1964.
(40) Sandeman, I. *Proc. R. Soc. London A* **1955**, 105.
(41) Cheam, T. C.; Krimm, S. *J. Chem. Phys.* **1985**, *82*, 1631.
(42) Moore, W. H.; Krimm, S. *Biopolymers* **1976**, *15*, 2439.
(43) Liang, R. C.; Lai, W. Y. F.; Reiser, A. *Macromolecules* **1987**, *20*, 2510.
(44) Elias, H. G. *J. Macromol. Sci., Chem.* **1973**, *A7*, 601.
(45) Lee, H. S.; Hsu, S. L. *Macromolecules* **1989**, *22*, 1100.

Registry No. MDI/BD/PPO (copolymer), 37205-91-7; MDT/BD/methyloxirane (copolymer), 71473-65-9; Au, 7440-57-5; glycerin, 56-81-5.